Reprinted from

Journal of Vacuum Science & Technology B

JVST B

Second Series
Volume 13, Number 6
Nov/Dec 1995

Nanobeam process system: An ultrahigh vacuum electron beam lithography system with 3 nm probe size

H. Hiroshima, S. Okayama, M. Ogura, and M. Komuro
Electrotechnical Laboratory, 1-1-4 Umezono, Tsukuba, Ibaraki 305, Japan

H. Nakazawa, Y. Nakagawa, K. Ohi, and K. Tanaka
JEOL Ltd., 1-2 Musashino, 3-chome Akishimna, Tokyo 196, Japan

pp. 2514-2517

An official journal of the American Vacuum Society
Published for the Society by the American Institute of Physics

Nanobeam process system: An ultrahigh vacuum electron beam lithography system with 3 nm probe size

H. Hiroshima, S. Okayama, M. Ogura, and M. Komuro
Electrotechnical Laboratory, 1-1-4 Umezono, Tsukuba, Ibaraki 305, Japan

H. Nakazawa, Y. Nakagawa, K. Ohi, and K. Tanaka
JEOL Ltd., 1-2 Musashino, 3-chome Akishimna, Tokyo 196, Japan

(Received 2 June 1995; accepted 10 August 1995)

We have constructed a "nanobeam process system" which is applicable to high resolution electron beam lithography using inorganic resists and is also compatible with electron beam induced surface reaction. It is a 50 kV electron beam lithography system with a gas introducible ultrahigh vacuum sample chamber using a double chamber stage system which isolates stage mechanisms from the sample chamber. The probe size measured with a knife edge method was 2.8 nm, where the probe current was 127 pA. The base pressure of the sample chamber was 3.5×10^{-7} Pa after baking. The pressure of the gun chamber did not vary at all and the pressure rise of the mechanism chamber was 3×10^{-6} Pa when the pressure of the sample chamber increased to 1×10^{-3} Pa during N_2 gas introduction. Standard deviations of stitching and overlay accuracy were 14 and 18 nm, respectively. Line patterns with a width of about 5 nm and a pitch of 15 nm were delineated in SiO_2 when used as a high resolution resist. © *1995 American Vacuum Society.*

I. INTRODUCTION

For electronic devices based on quantum effects or Coulomb blockade phenomenon, reduction of feature sizes is a requirement for demonstration of these functions at higher temperature. Electron beam (EB) lithography in which 10–20-nm-wide patterns are delineated using organic resists[1] is thought to be one of the most promising tools for such nanofabrication. Inorganic resists such as metal oxides and metal halides are candidates for higher resolution resists.[2,3] However, contamination grown during EB exposure in a low vacuum prevents self-development of sublimation-type materials or reduces the resolution by scattering electrons. If the vacuum around the sample is high enough, EB-induced surface reactions such as direct etching of target materials and deposition of metals can be also realized by the introduction of appropriate gases.[4,5] Those materials and processes are attractive because the minimum fabrication size can be defined by the size of the probe beam. However, it is difficult to apply a conventional EB direct writer to those processes by baking to reduce the base pressure, as the high precision of a stage mechanism will be degraded after baking. Thus, we constructed a nanobeam process system with an ultrafine probe and a gas introducible ultrahigh vacuum (UHV) sample chamber with a double chamber stage system[6] to be compatible with these high resolution processes.

II. SYSTEM DESIGN

A. Electron optics

Figure 1 shows the schematic view of the nanobeam process system. A ZrO/W thermal field emitter and a triplet lens system with a zoom function were adapted.[7] High beam voltage is preferable in order to reduce a chromatic aberration, diffraction, and beam broadening in a target by forward scattering. We selected an acceleration voltage of 50 kV, considering the reliability of the high voltage system. The gun lens is an electrostatic lens and the others are electromagnetic lenses. The total aberrations of the system are mainly defined by the objective lens when the objective lens operates at a low magnification. Thus, an objective lens with low aberration coefficients was designed for fine focusing and retrofitted to a commercial EB lithography system (JEOL JBX-6000FS) for efficient development. The working distance and the optical path which were minimized as much as possible are 16 and 381 mm, respectively. The total magnification, and spherical and chromatic aberration coefficients are 0.024, 43.8 mm, and 16.1 mm, respectively. The probe diameter as a function of the beam convergent half-angle was calculated and is given in Fig. 2, where it was assumed that the source size and the energy spread of emitted electrons were 30 nm and 1 eV,[8] respectively. The minimum calculated probe diameter is 2.5 nm at the optimum convergent half-angle of 3.7 mrad and a corresponding probe current is 120 pA when an emitter operates with an angular current density of 0.5 mA/sr at an extraction voltage of 5 kV.

B. Ultrahigh vacuum sample chamber

A schematic view of the developed double chamber stage system is shown in Fig. 1. The sample chamber excludes most parts of the stage mechanism such as mirrors, stage guides, bearings, and so on. The stage moves while maintaining a gap between the moving plate (hatched part in Fig. 1) and the stationary plate of 0.3 mm. The inner diameter of the latter is 230 mm and the minimum overlap length of the gap is 70 mm. The calculated conductance of the gap is 0.6 ℓ/s, which corresponds to that of an orifice with a diameter of 0.25 mm and enables differential evacuation. A retractable gas injection nozzle is attached, which is adjusted a few tenths of a mm above the sample, in order to produce a high gas flux with a small gas flow for EB-induced surface reaction. Note that the gap prevents not only the residual gases in the mechanism chamber from diffusing into the sample

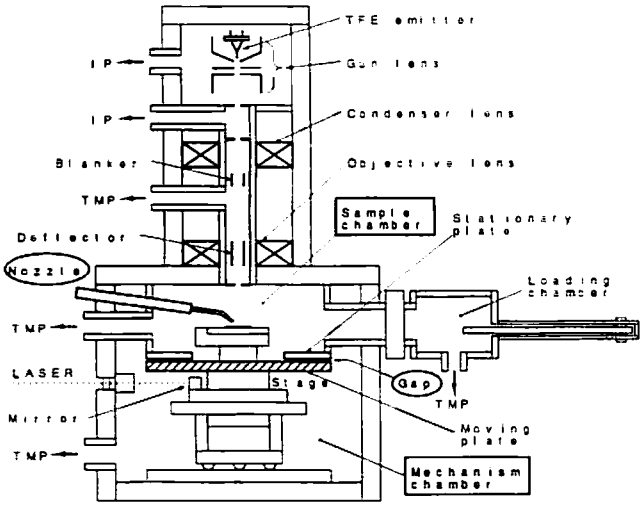

FIG. 1. Schematic view of the nanobeam process system with a double chamber stage system.

chamber, but also the process gases in the sample chamber from diffusing into the mechanism chamber in the case of EB-induced surface reactions. By adapting a double chamber stage system, we can use reliable stage mechanisms without being concerned about reduction of the precision by baking or requiring chemical protection.

C. Total system

The optical column is separated with orifices into several chambers which are evacuated by independent pumps. The sample chamber and the two neighboring chambers are evacuated with chemical proof turbo molecular pumps through vibration dampers. A sample is exchanged through the loading chamber without breaking the vacuum of the sample chamber. Available sample sizes are a 2 in. wafer and a 10 mm square piece wafer. The maximum field size is 80 μm×80 μm and the minimum scanning increment is 2.5 nm.

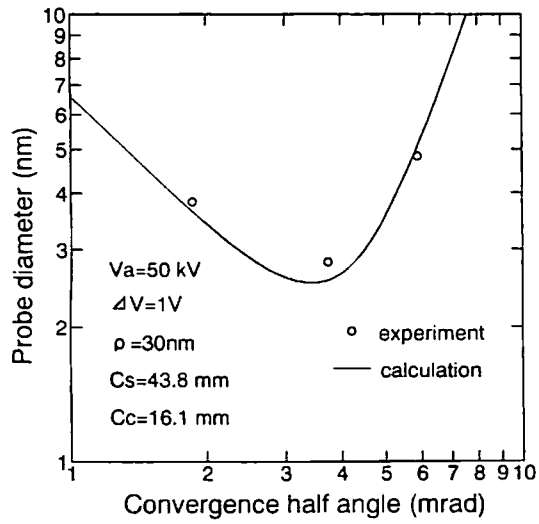

FIG. 2. Probe diameter as a function of the convergent half-angle.

TABLE I. Principal specifications.

Acceleration voltage	50 kV
Cathode	ZrO/W TFE
Probe diameter and current	3 nm at 100 pA
Minimum scanning increment	2.5 nm
Maximum scanning rate	6 MHz
Field size	80 μm×80 μm
Laser resolution	5 nm
Stitching accuracy	20 nm (σ)
Overlay accuracy	20 nm (σ)
Substrate size	2 in., 10 mm sq.
Base pressure of sample chamber	3.5×10^{-7} Pa
Allowable gas flow	$<10^{-4}$ Pa m^3/s

The stage position is monitored with a laser measuring system with a resolution of 5 nm. A laser feedback, which cancels the displacement of a real stage position to the ideal one, is activated either in real time or at intervals. The software for exposure is basically same as that of a standard JBX-6000FS EB lithography system except that the status of the nozzle position is checked and the travel area of the stage is restricted in order not to crush it. The optical column and most of control units are set in a clean room with a temperature stability of ±0.1 °C. The principal specifications are summarized in Table I.

III. SYSTEM PERFORMANCE

The probe diameter was measured by a knife edge method. A Au coated Ni mesh was used as a knife edge and a $p-n$ junction detector was located underneath. By scanning the probe beam across the edge, the current profile of the probe beam was measured. The probe diameter was determined by a scanning distance where the detected current varying from 15% to 85% of the maximum value. Typical results are shown in Fig. 3. A stigmatic probe beam with a diameter of 2.8 nm and the probe current of 127 pA was obtained for a convergent half-angle of 3.74 mrad. The measured probe diameters for three different convergent half-angles are plotted in Fig. 2, where the data represent the minimum value of many trials, since the poor edge condition

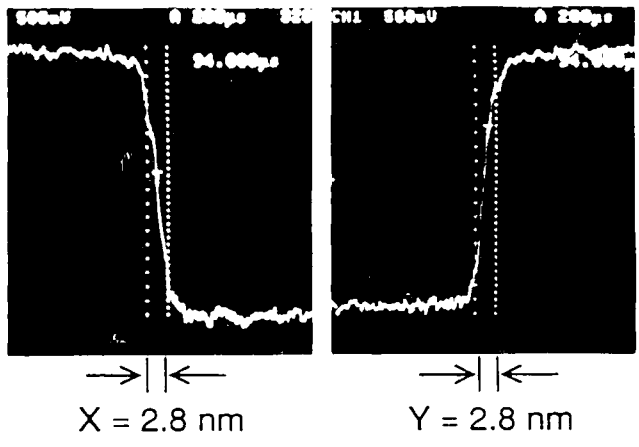

FIG. 3. Probe diameter measured by a knife edge method. The acceleration voltage and the probe current are 50 kV and 127 pA, respectively.

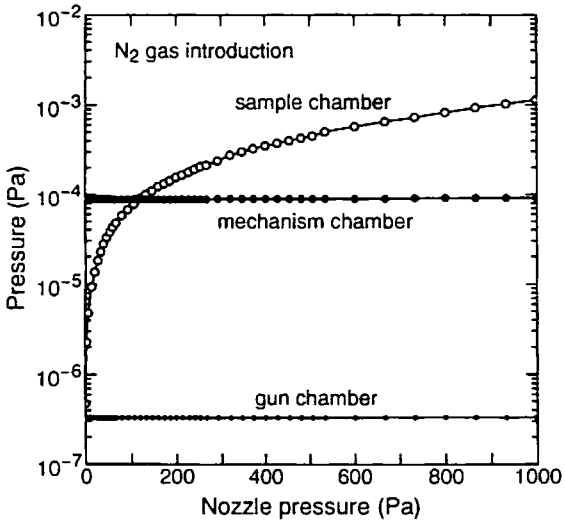

FIG. 4. Variation of pressures during gas introduction.

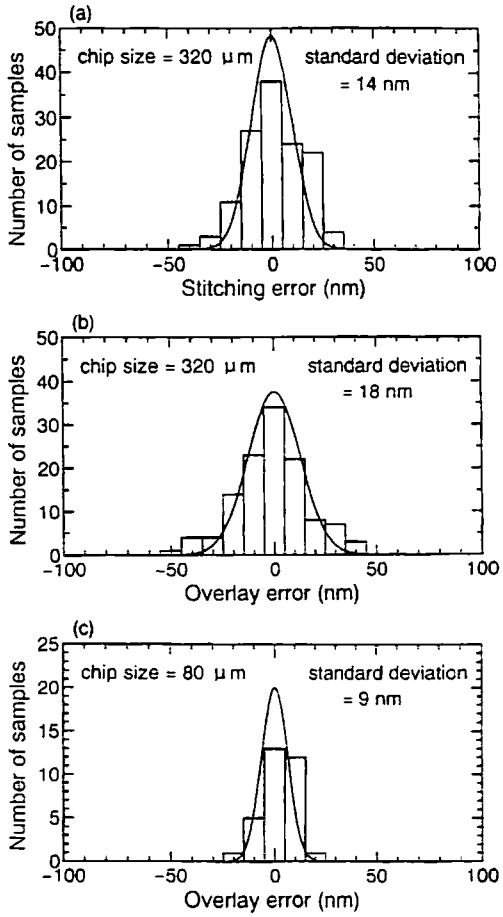

FIG. 5. Stitching and overlay accuracy. (a) Stitching; (b) overlay; (c) overlay for a pattern smaller than a field size.

enlarges the measured probe diameter. The experimental results agree with the calculation well, thus it is concluded that the optical column operates as designed.

The sample chamber was baked at 245 °C with built-in panel heaters for 48 h, while the temperature of the stage top was raised less than 50 °C. The pressure after baking was 3.5×10^{-7} Pa, which is two orders of magnitude smaller than that of a conventional EB lithography system. It is not necessary to follow such a baking procedure to the exchange of samples. The changes in pressure of the gun chamber and the mechanism chamber during gas introduction are shown in Fig. 4. In this experiment, N_2 gas was introduced into the sample chamber by varying the pressure of the gas injection nozzle. When a pressure of the sample chamber became 1×10^{-3} Pa, that of the gun chamber was not varied at all and the variation of that of the mechanism chamber was 3×10^{-6} Pa. Thus, it is expected that the emitter and the stage mechanism will operate without trouble in the case of EB-induced surface reaction processes using reactive gases.

Stitching and overlay accuracy was measured by exposing a test pattern at 15 locations on a PMMA resist. The test pattern was a 320 μm×320 μm area with scales and verniers with a resolution step of 10 nm. The deviations at the same portion of different chips were evaluated by scanning electron microscopy (SEM) inspection. The results of 120 locations are shown in Figs. 5(a) and 5(b). The standard deviations of stitching and overlay are 14 and 18 nm, respectively. Relatively good results were obtained, however they are somewhat inferior to the values of a standard JBX-6000FS. As the sample is not in the plane of the laser beam paths in our EB lithography system (see Fig. 1), a pitch of the stage changes the sample position even if the measured position with the laser measuring system is not changed. The degradation of precision may be caused by such a phenomenon. However, this will not be a serious problem for our purpose, because the exposure area of the key portion of nanodevices is probably smaller than the field size of 80 μm×80 μm in most cases. If a pattern is so small that markers for overlay are included in a field, overlay accuracy is improved to 9 nm as shown in Fig. 5(c).

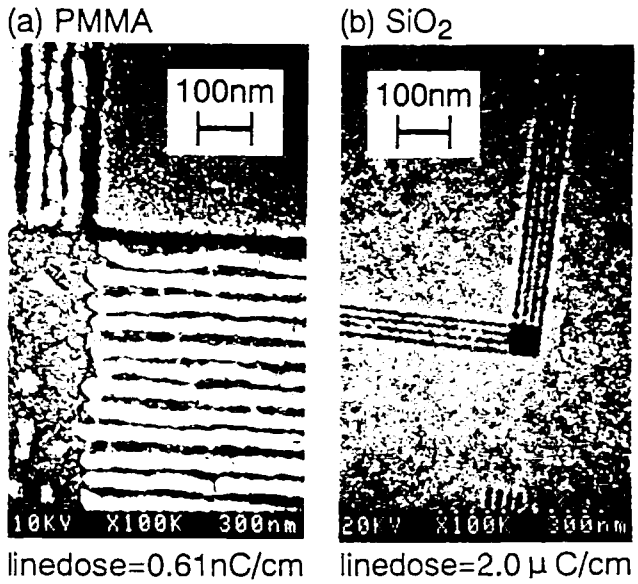

FIG. 6. SEM images of delineated line patterns. (a) 40 nm pitch lines in PMMA and (b) 15 nm pitch lines in SiO_2 as a high resolution resist.

Fine patterning tests were carried out on a 30-nm-thick PMMA resist spun on a Si wafer and a 20-nm-thick SiO_2, where the beam voltage was 50 kV and the probe current was about 100 pA. The PMMA was developed using 1:3 MIBK:IPA at 22 °C for 60 s and coated with Au/Pd for SEM inspection. The SiO_2 was exposed in O_2 plasma and dipped in a buffered HF solution of which the concentrations of HF and NH_4F are 0.2 mol/ℓ, for 100 s.[9] Figure 6 shows SEM images of the delineated lines with a pitch of 40 nm in PMMA [Fig. 6(a)] and with a pitch of 15 nm in SiO_2 [Fig. 6(b)]. The width of developed lines in PMMA fluctuate and the residuals between lines were broken as shown in Fig. 6(a). We think that a clearer pattern can be obtained by adjusting coating and developing processes, since the resolution limit of PMMA is somewhat higher[10] and smooth and fine lines were developed in SiO_2 as shown in Fig. 6(b). The linewidth of patterns with a 15 nm pitch is estimated about 5 nm by the ratio of a width of the dark contrast line to that of the bright one, where the exposure was carried out without a laser feedback in real time.

IV. SUMMARY

We designed a nanobeam process system which is compatible with inorganic resist exposure and EB-induced surface reaction processes. The UHV sample chamber coexists with the precision stage system by using a double chamber stage system. The base pressure of the sample chamber was 3.5×10^{-7} Pa and the system is expected to endure the EB-induced surface reaction process using reactive gases. An electron beam with a probe diameter of 2.8 nm and a probe current of 127 pA is available at 50 kV. The performance was achieved with only a minor tradeoff in high accuracy of stitching and overlay. Line patterns with a width of about 5 nm and a pitch of 15 nm were fabricated in SiO_2 as a high resolution resist.

ACKNOWLEDGMENT

The authors would like to acknowledge the continual encouragement from Tsunenori Sakamoto at the Electrotechnical Laboratory.

[1]A. N. Broers, J. Electrochem. Soc. **128**, 166 (1981).
[2]X. Pan and A. N. Broers, Appl. Phys. Lett. **63**, 1441 (1993).
[3]I. G. Salisbury, R. S. Timsit, S. D. Berger, and C. J. Humphreys, Appl. Phys. Lett. **45**, 1289 (1984).
[4]Y. Sugimoto, K. Akita, M. Taneya, and H. Hidaka, Appl. Phys. Lett. **57**, 1012 (1990).
[5]S. Matsui and K. Mori, J. Vac. Sci. Technol. B **4**, 299 (1986).
[6]S. Okayama, M. Ogura, M. Komuro, and H. Hiroshima, Japan Patent No. 5-90792 (1993); U.S. Patent No. 8-206161 (1993); German Patent No. P4408523.0; Dutch Patent No. 94.00393.
[7]H. Hiroshima *et al.*, Nucl. Instrum. Methods A **363**, 73 (1995).
[8]L. W. Swanson, *Electron Optical Systems* (SEM, Chicago, 1984), p. 137.
[9]H. Hiroshima and M. Komuro, Jpn. J. Appl. Phys. **32**, 6153 (1993).
[10]W. Chen and H. Ahmed, Appl. Phys. Lett. **62**, 1499 (1993).